PCCP

PAPER

View Article Online
View Journal | View Issue

Cite this: *Phys. Chem. Chem. Phys.*, 2016, **18**, 22687

Functionalization effect on a Pt/carbon nanotube composite catalyst: a first-principles study

Byung-Hyun Kim,[ab] Kwang-Ryeol Lee,[a] Yong-Chae Chung[b] and Mina Park*[a]

Received 15th December 2015,
Accepted 18th July 2016

DOI: 10.1039/c5cp07737k

www.rsc.org/pccp

Chemical interactions between Pt and both pristine and defective carbon nanotubes (CNTs) that were functionalized with various surface functional groups, including atomic oxygen (–O), atomic nitrogen (–N), hydroxyl (–OH) and amine ($–NH_2$) groups, were investigated through first-principles calculations. Our calculations suggest that the oxygen or nitrogen of the surface functional group can promote better structural stability of a Pt/CNT complex in terms of the binding energy enhancement between Pt and CNTs. Enhanced binding of the Pt/CNT complex would improve the long-term durability of the complex and thus enhance the catalytic activity of Pt catalysts supported on CNTs. Among the functional groups investigated, atomic nitrogen resulted in the most consistent increase in the Pt binding energies on pristine or defective CNTs. Moreover, atomic nitrogen decoration on the surface of CNTs rather than substitution into the CNTs appears to be more desirable. A d-band centre analysis and H_2 adsorption calculations also revealed that the catalytic activity of Pt can be improved *via* efficient functionalization of the CNT support.

Introduction

Recently, due to their unique mechanical and electrical properties, nanostructured carbon materials such as carbon nanotubes (CNTs) or graphene have attracted much attention due to their potential applications in many research areas, *e.g.* as building blocks in nanoelectronics and spintronic devices and as a support for catalysis and fuel cell electrocatalysis.[1–13] For example, CNTs have been regarded as promising candidates for catalytic supports in various fuel cells due to their mechanical stability and large surface area. Many experimental studies have revealed that Pt catalysts that are supported on CNTs achieved better catalytic activity than those supported on conventional carbon black.[14,15] One major issue for CNT-supported catalysts is that the surface of pristine CNTs is chemically inert; therefore, the binding energy between pristine CNTs and Pt particles is weak, which results in the aggregation of Pt nanoparticles into larger particles and, hence, degradation of their catalytic activity.[16] Therefore, an understanding of the binding characteristics necessary to improve the interfacial strength between CNTs and Pt becomes crucial to control the stability and catalytic activity of Pt catalysts that are supported on CNTs for real applications.

Many efforts have been made to understand the interaction mechanism of Pt atoms at CNT surfaces. Several theoretical investigations have reported the adsorption energies and the atomic and electronic structures of Pt atoms interacting with pristine or defective CNTs.[17–21] However, previous studies were limited by the lack of consideration of the surface functionalization of CNTs, although most CNT applications involve a surface treatment process to promote uniform dispersion and/or functionalization of the CNT surface, which would decorate the CNT surfaces with various functional groups. Moreover, Collins *et al.* reported that the electronic properties of CNTs, including the local density of states, are sensitive to the chemical environment,[22] so any functionalization on the CNT surface should influence the chemical properties of the CNTs and thus affect the binding mechanism at the Pt/CNT interface. Consequently, it is imperative to investigate the interaction of Pt atoms with functionalized CNTs. Recently, Hu and co-workers reported experimental and theoretical investigations which show that Pt nanoparticles were immobilized on nitrogen-doped CNTs since nitrogen incorporation efficiently enhanced the binding energy of Pt on nitrogen-doped CNTs, resulting in better catalytic activity for oxygen reduction and methanol oxidation reactions.[21] Zhang *et al.* investigated the catalytic activity of Pt nanoparticles on CNTs functionalized with amine or carboxyl groups and suggested that Pt/CNTs functionalized with an amine group exhibited significantly enhanced oxygen reduction reaction activity due to their higher electrochemical durability compared to that of a carboxyl group.[8] However, further investigations are required to reveal the mechanism that improved the structural stability of Pt/CNTs functionalized by various chemical environments.

Herein, we theoretically investigate the chemical interaction between Pt and functionalized CNT surfaces based on the

[a] *Computational Science Research Center, Korea Institute of Science and Technology, 5, Hwarang-ro 14-gil, Seongbuk-gu, Seoul 02792, Republic of Korea. E-mail: dreamer@postech.ac.kr*
[b] *Department of Materials Science Engineering, Hanyang University, 222 Wangsimni-ro, Seongdong-gu, Seoul 04763, Republic of Korea*

density functional theory calculations in addition to a d-band centre analysis and H_2 molecule adsorption on the Pt/CNT complexes. We focused on how functional groups that include oxygen and nitrogen affect the binding energy of Pt by examining the interaction behaviour of a single Pt atom adsorbed on the outer surfaces of various CNTs with and without four different functional groups: atomic oxygen (–O), atomic nitrogen (–N), hydroxyl (–OH) and amine ($–NH_2$) groups, which are most frequently observed during CNT growth or after the chemical treatment that is widely used in CNT applications.[23–25] Our results show that the binding energy between Pt and CNTs can be enhanced by the surface functionalization of CNTs, especially by atomic nitrogen decoration on the CNT surface. By combining a d-band centre analysis and H_2 adsorption calculations, we found that the catalytic activity of the Pt/CNT composite catalyst can be modified by choosing different functional groups.

Calculation details

First-principles calculations of the total energies, geometry optimization and electronic structures for pristine and topologically defective CNTs with various functional groups and their complexes with the adsorption of a single Pt atom have been performed using the SIESTA code[26,27] based on spin-resolved density functional theory. We adopted the generalized gradient approximation (GGA) of Perdew, Berke and Ernzerhof (PBE)[28] for the exchange–correlation energy functional and standard norm-conserving pseudopotentials generated according to the procedure of Troullier and Martins to describe the ion–electron interactions.[29] A split-valence double-ζ plus polarization function (DZP) basis set was employed with an energy cutoff of 150 Ry.

We examined the dependence of the binding behaviour of a Pt atom on the functional groups at the CNT surfaces. (6,6) armchair CNTs with 5 unit cells in the z-direction were used for our calculations. To evaluate the interactions between (functionalized) CNTs and Pt, the binding energies, E_b, of Pt were calculated by

$$E_b = E_{tot}[\text{(functionalized) CNT + Pt}] - E_{tot}[\text{(functionalized) CNT}] - E_{tot}[\text{Pt}], \quad (1)$$

where E_{tot} is the total energy of the system. The binding energies were corrected using the basis set superposition error (BSSE) correction through the counterpoise method with ''ghost'' atoms.[30] Negative E_b values denote an exothermic binding process.

In this study, periodic boundary conditions were applied along the tube axis (z-direction) to simulate one-dimensional infinite nanotubes. In the lateral (x, y) directions, vacuum regions were approximately 15 Å to avoid image–image interactions between neighbouring supercells with eight k-points generated by the Monkhorst–Pack scheme along the tube axis.[31] All atom positions in the supercell were fully relaxed without any constraints using the conjugate-gradient algorithm, and the convergence threshold was set at 0.04 eV $Å^{-1}$ for the forces on each atom.

Results and discussion

Table 1 summarizes the calculation results of the present work: nearest-neighbour distances between Pt and the carbons, the equilibrium distance between Pt and the functional groups ($d_{Pt–X}$), the binding energies of the atomic Pt adsorbed on the (functionalized) CNTs, and the average energy of the d electrons (d-band centre) of a Pt atom. Note that we considered a single Pt atom even though Pt nanoparticles are used as the metal catalyst in real experiments. Thus, the calculated binding energies of a single Pt atom would be larger than those of Pt nanoparticles since no Pt–Pt interactions are included in the adsorption of a single Pt atom. However, our aim of this work is to investigate the effects of functional groups on the binding energies of a Pt atom adsorbed on the CNTs. Our results can provide useful information which shows the interaction behaviour of a Pt atom with CNTs functionalized in various chemical environments.

Pt adsorption on various CNTs without functional groups

The calculated binding energy of a single Pt atom on the surface of pristine CNTs (P-CNT) was −1.57 eV, which is consistent with the previous first-principles calculation results.[17] After geometry optimization, the Pt atom was found to be at the bridge site on the CNT with a Pt–C distance of 2.05 Å, as shown in Fig. 1(a). The projected partial density of states (PDOS) for the Pt and C atoms on CNTs shows a very weak hybridization between the Pt 5d and C 2p orbitals (Fig. 1(d)). It is well known that any defects on CNTs can enhance the adsorption of a metal atom due to the increased reactivity of carbon atoms near the defects.[18,32] For Pt adsorption on the Stone–Wales CNT (SW-CNT), the calculated binding energy was increased to −2.29 eV. As shown in Fig. 1(b), Pt tends to bond to the site above the C–C bond between two pentagons. The bond lengths of Pt–C were 2.04 Å, similar to those for Pt on the P-CNT. Our PDOS analysis revealed that the improved binding energy is attributed to hybridization between

Table 1 Nearest-neighbour distances between Pt and the carbon(s) ($d_{Pt–C}$), the equilibrium Pt-functional group distance ($d_{Pt–X}$) for the (functionalized) CNTs, the binding energies of the atomic Pt adsorbed on the (functionalized) CNTs (E_b), and the average energy of the d electrons (d-band centre) of a Pt atom

	$d_{Pt–C}$ (Å)	$d_{Pt–X}$ (Å)	E_b (eV)	E_{dc} (eV)
Pt/P-CNT	2.05/2.05	—	−1.57	−1.75
Pt/P-CNT-O	2.06/2.04	3.65	−2.19	−1.80
Pt/P-CNT-N	2.14/2.14	2.12	−3.26	−2.71
Pt/P-CNT-OH	2.04/2.10	2.13	−2.43	−1.79
Pt/P-CNT-NH_2	2.06	2.19	−2.07	−2.27
Pt/SW-CNT	2.04/2.04	—	−2.29	−1.96
Pt/SW-CNT-O	1.98/2.31	2.05	−2.90	−2.34
Pt/SW-CNT-N	2.06/2.55	1.88	−3.37	−3.02
Pt/SW-CNT-OH	2.06/2.03/2.49	2.99	−2.54	−1.93
Pt/SW-CNT-NH_2	2.10/2.10	2.33	−2.70	−1.98
Pt/MV-CNT	1.92/1.92/2.00	—	−5.77	−5.08
Pt/MV-CNT-O	2.15/2.10	2.14	−2.25	−2.64
Pt/MV-CNT-N	2.04/2.05	2.89	−2.36	−1.89
Pt/MV-CNT-OH	2.17/2.09/2.10	3.23	−2.12	−2.15
Pt/MV-CNT-NH_2	1.98/2.18/2.03	2.47	−3.27	−3.15

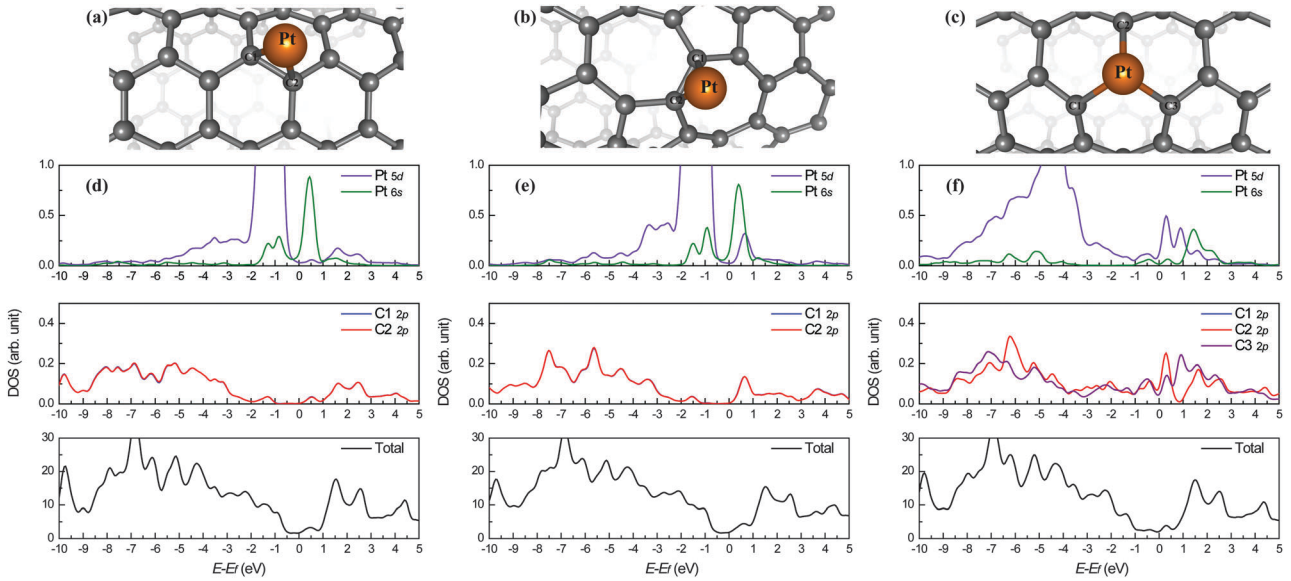

Fig. 1 Energy-minimized structures and the density of states for Pt adsorption on pristine and defective CNTs: (a and d) Pt/P-CNT, (b and e) Pt/SW-CNT, and (c and f) Pt/MV-CNT. The orange ball represents the Pt atom, and the grey balls represent the carbon atoms.

the Pt 5d and C 2p orbitals at the deep level of around −6 eV (Fig. 1(e)). For the monovacancy CNT (MV-CNT), the calculated binding energy was significantly enhanced to −5.77 eV; the Pt atom was observed to strongly bond to the vacancy site and saturate the dangling bonds of the C atoms near the defect site *via* a very strong hybridization of the Pt 5d orbital with the C 2p orbital in the Pt/MV-CNT (Fig. 1(f)). When a monovacancy defect is created in the CNTs, the three active dangling bonds surrounding the defect rearrange to form a pentagon–enneagon structure, which leaves only one dangling carbon. However, we observed that Pt adsorption at the vacancy site caused a return of its atomic configuration to the original triangular form with Pt in the centre with a shorter bond distance of Pt–C ranging from 1.92 to 2.0 Å, as shown in Fig. 1(c). Nevertheless, direct adsorption of Pt on the defects, as described above, is hardly expected due to the high reactivity of the defective carbons under ambient conditions. Usually, these defects would be healed by adsorbing molecules from the ambient atmosphere or during the chemical treatment of the CNTs. Nitrogen-containing molecules are frequently observed when a single-walled CNT is grown under a nitrogen atmosphere, whereas oxygen-containing functional groups are usually found after a strong acid treatment process, which is widely used in CNT applications.[23–25]

Pt adsorption on various CNTs with –O and –N functional groups

Both –O and –N functional groups enhanced the binding energy of a Pt atom on the P-CNT to values of −2.19 eV and −3.26 eV, respectively. It was observed, as shown in Fig. 2(a), that the Pt atom preferred to bind with the C atoms that do not bind to the O atom in the –O functionalized P-CNT. However, the Pt atom was observed to directly bind to the N atom with a bond length of 2.12 Å, which resulted in a higher binding energy due to the strong hybridization between the Pt 5d and N 2p orbitals in the –N functionalized P-CNT, as shown in Fig. 2(b and d). For the SW-CNT shown in Fig. 3, it was also revealed that both functional groups could enhance the binding energy to values of −2.90 and −3.37 eV for –O and –N functionalized SW-CNTs, respectively; this increase was even greater than in the cases of the P-CNT because the Pt atom preferred to directly bind to the functional groups for both –O and –N functionalized SW-CNTs. In particular, for Pt/SW-CNT-N, we observed that the Pt 5d orbital was strongly hybridized with the C 2p and N 2p orbitals.

However, for the MV-CNT, we obtained relatively low (−2.25 and −2.36 eV) binding energies for both the –O and –N functional groups compared to the other cases (Fig. 4). As shown in Fig. 4(a)

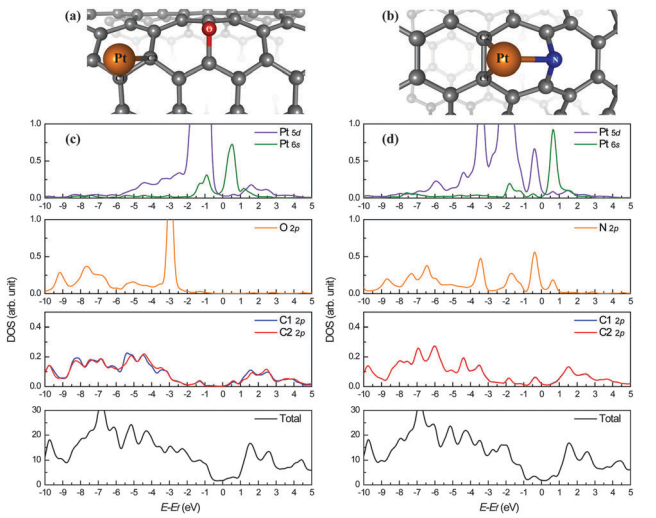

Fig. 2 Energy-minimized structures and the density of states for Pt adsorption on functionalized pristine CNTs with atomic oxygen and nitrogen: (a and c) Pt/P-CNT-O and (b and d) Pt/P-CNT-N. The red ball represents the O atom, and the blue ball represents the N atom.

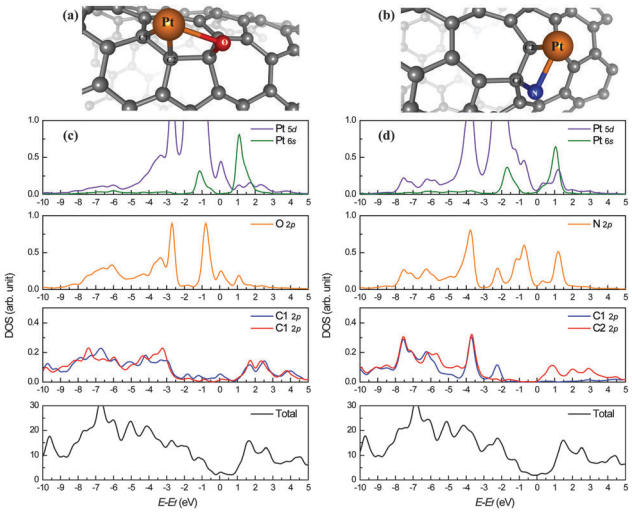

Fig. 3 Energy-minimized structures and the density of states for Pt adsorption on functionalized Stone–Wales defective CNTs with atomic oxygen and nitrogen: (a and c) Pt/SW-CNT-O and (b and d) Pt/SW-CNT-N.

for Pt/MV-CNT-O, it was observed that the O atom saturated the carbon atom, which had one dangling bond in the enneagon ring, then bound to the Pt atom located on the pentagon carbon ring. However, when a N atom was incorporated into the MV-CNT shown in Fig. 4(b), the N atom was located at the vacancy site and saturated the dangling bonds of the C atoms near the defect site, which was analogous to N doping in CNTs. Our calculations show that the Pt atom was observed to bind with the C atoms near the –N functional atom instead of binding directly to the N atom. From the PDOS analysis in Fig. 4(d), the contribution of the N 2p orbital to the Pt adsorption in the –N functionalized MV-CNT was observed to be negligible compared to those in –N functionalized pristine and/or SW-CNTs, as mentioned above.

However, it is known that N incorporation into the CNTs results in the activation of neighbouring carbon atoms due to the high electron affinity of nitrogen; thus, the N atom promotes the binding energy enhancement of the Pt atom on the –N functionalized MV-CNT.[19] Consequently, our result showed that an –N functional atom can promote better structural stability of a Pt/CNT composite catalyst, which is consistent with the experimental observation that the doping of N into CNTs demonstrated long-term durability.[11] Moreover, we suggest that the N atom decoration on the CNTs would be more desirable than substitution in terms of the binding energy enhancement between Pt and the CNTs.

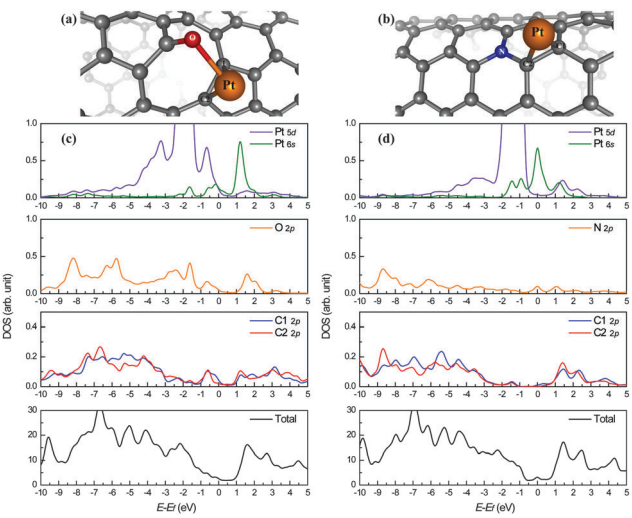

Fig. 4 Energy-minimized structures and the density of states for Pt adsorption on functionalized monovacancy defective CNTs with atomic oxygen and nitrogen: (a and c) Pt/MV-CNT-O and (b and d) Pt/MV-CNT-N.

Pt adsorption on various CNTs with –OH and –NH_2 functional groups

We also considered –OH and –NH_2 functional groups because both atomic O and N atoms can be easily hydrogenated by capturing H atoms under any experimental conditions. It is noted that the –OH and –NH_2 functional groups retained their molecular structure without dissociation after Pt adsorption on the functionalized CNTs for all the cases under our simulation conditions. As shown in Fig. 5, a Pt atom bound to CNTs at a distance from the –OH functional groups, whereas the –NH_2 functional groups acted as a bridge between the Pt atom and CNTs for both the pristine and defective CNTs. The binding energies of a Pt atom on –OH or –NH_2 functionalized P- or SW-CNTs were found to be −2.43 eV, −2.07 eV, −2.54 eV, and −2.70 eV for P-CNT-OH, P-CNT-NH_2, SW-CNT-OH, and SW-CNT-NH_2, respectively; these values were lower than the values for the –O and –N functional groups (see Table 1) because the –OH or –NH_2 functional groups showed a reduced chemical activity due to electron deprivation by hydrogen. Moreover, Pt adsorption on –OH functionalized CNTs exhibited higher binding energies than that on –NH_2 functionalized CNTs even though the Pt atom was directly bonded to NH_2 and CNTs. However, the Pt/MV-CNT-NH_2 complex showed a remarkably enhanced binding energy (−3.27 eV).

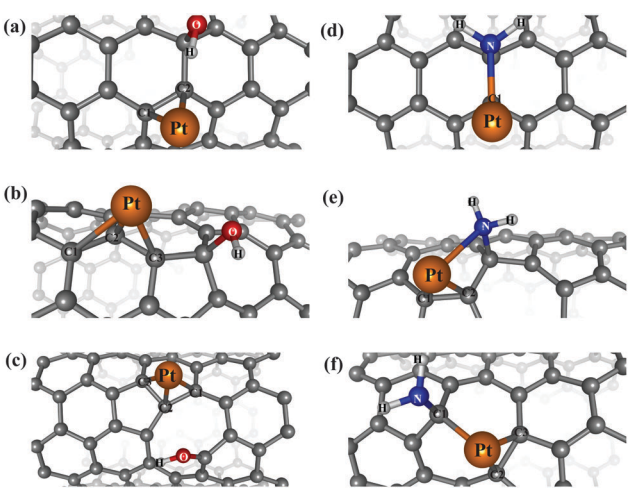

Fig. 5 Energy-minimized structures of Pt adsorption on functionalized CNTs with hydroxyl and amine: (a) Pt/P-CNT-OH, (b) Pt/SW-CNT-OH, (c) Pt/MV-CNT-OH, (d) Pt/P-CNT-NH_2, (e) Pt/SW-CNT-NH_2, and (f) Pt/MV-CNT-NH_2. The white balls represent the H atoms.

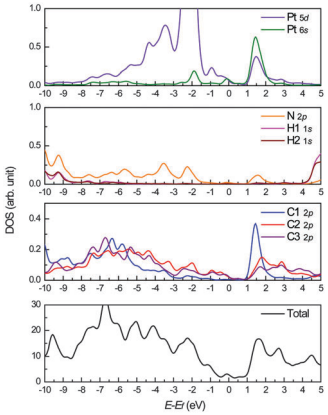

Fig. 6 The density of states for Pt/MV-CNT-NH_2. The carbon and hydrogen atom indices correspond to the carbon and hydrogen atoms in the configuration in Fig. 5(f).

From our PDOS analysis, it can be deduced that the bonding of the $-NH_2$ functional group with C1 caused a weakening of the carbon–carbon interaction in a hexagon ring, resulting in the C1 atom becoming more reactive, so that a strong hybridization between the C1 2p and Pt 5d orbitals was observed (Fig. 6).

Stability of functional groups

The binding energies of functional groups on various CNTs were also calculated and summarized in Table 2 in order to make sure that the functionalized CNTs considered in this work are still stable even after Pt adsorption. For both –O and –N functional groups, it showed that the binding energies of functional groups were higher than those of Pt adsorption on CNTs. It indicates that the substitution of the Pt atom for functional groups attached on CNTs, *i.e.*, direct adsorption on CNTs (−1.57 eV for Pt/P-CNT, −2.29 eV for Pt/SW-CNT, and −5.77 for Pt/MV-CNT) is found to be energetically unfavourable. On the other hand, the binding energies of the –OH and $-NH_2$ functional groups were found to be slightly lower or comparable to the direct adsorption of the Pt atom. However, it is worth noting that the functional group attachment occurs during the surface treatment process which is performed prior to Pt deposition in most experiments.[5,8–11,16,24] Therefore, we assume that Pt substitution for functional groups is hardly expected in this work.

Catalytic activity variation

It is known that the average energy of the d electrons (called the d-band centre) of a Pt atom is highly correlated with the catalytic activity for oxygen and hydrogen adsorption. When the d-band centre is close to the Fermi energy, antibonding states are shifted up and become empty states, whereas bonding states are shifted down and become occupied states; as a result, the oxygen and hydrogen adsorption energies increase.[33,34] Table 3 and Fig. 7 show the calculated H_2 adsorption energies on various Pt/CNT composite catalysts with respect to the d-band centre of a Pt atom on the functionalized CNTs. We found a linear dependence of the adsorption energy of H_2 in various Pt/CNT complexes with the d-band centre of a Pt atom. The higher binding energy of the H_2 molecule with various CNTs indicates that the d-band centre is closer to the Fermi energy. It can be concluded that the electronic structure of the Pt/CNT surface, and hence the catalytic activity, can be controlled by introducing different functional groups.

Table 2 The binding energies of atomic oxygen and nitrogen, hydroxyl and amine functional groups on the various CNTs

	O (eV)	N (eV)	OH (eV)	NH_2 (eV)
P-CNT	−5.27	−2.16	−1.53	−0.83
SW-CNT	−5.10	−2.09	−2.30	−1.61
MV-CNT	−8.21	−9.65	−4.22	−3.92

Table 3 The adsorption energies of the H_2 molecule on the various Pt/CNT composite catalysts

	None	–O	–N	–OH	$-NH_2$
P-CNT	−1.60	−1.50	−0.80	−1.60	−1.33
SW-CNT	−1.50	−1.31	−0.69	−1.49	−1.98
MV-CNT	−1.06	−1.62	−1.45	−1.51	−0.53

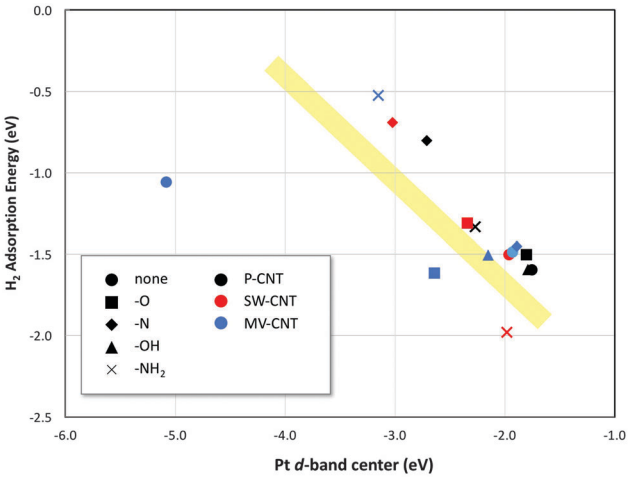

Fig. 7 The calculated H_2 adsorption energy with respect to the d-band centre of a Pt atom on pristine and defective CNTs with various functional groups.

Conclusions

The binding energies and electronic structures of various Pt/CNT complexes composed of a single Pt atom and pristine or defective CNTs functionalized with atomic oxygen and nitrogen, hydroxyl and amine groups were investigated through first-principles calculations. Our calculations showed that chemically active oxygen or nitrogen on functionalized CNT surfaces can be a promising candidate as the fabricating agent of a Pt/CNT composite catalyst to promote better structural stability. Moreover, our calculations suggest that atomic nitrogen decoration on the surface of CNTs rather than substitution into CNTs would be more desirable in terms of the binding

energy enhancement between Pt and CNTs. Analysis of H_2 adsorption on various Pt/CNT complexes with respect to the d-band centre of a Pt atom clearly shows a linear dependence, which indicates that the catalytic activity of the Pt/CNT composite catalyst can be controlled by introducing different functional groups.

Acknowledgements

The present work was supported by the KIST Fundamental Research Program, contract number 2E25372.

References

1 P. M. Ajayan and J. M. Tour, *Nature*, 2009, **447**, 1066.
2 W. Q. Deng, Y. Matsuda and W. A. Goddard III, *J. Am. Chem. Soc.*, 2007, **129**(32), 9834.
3 S. J. Tans, R. M. Verschueren and C. Dekker, *Nature*, 1998, **393**, 49.
4 J. M. Planeix, N. Coustel, B. Coq, V. Brotons, P. S. Kumbhar, R. Dutartre, P. Geneste, P. Bernier and P. M. Ajayan, *J. Am. Chem. Soc.*, 1994, **116**(17), 7935.
5 P. Serp, M. Corrias and P. Kalck, *Appl. Catal., A*, 2003, **253**(2), 337.
6 F. Peng, L. Zhang, H. Wang, P. Lv and H. Yu, *Carbon*, 2005, **43**(11), 2405.
7 L. Dennany, P. Sherrell, J. Chen, P. C. Innis, G. G. Wallace and A. I. Minett, *Phys. Chem. Chem. Phys.*, 2010, **12**, 4135.
8 S. Zhang, Y. Shao, G. Yin and Y. Lin, *J. Mater. Chem.*, 2010, **20**, 2826.
9 Z. Liu, X. Lin, J. Y. Lee, W. Zhang, M. Han and L. M. Gan, *Langmuir*, 2002, **18**, 4054.
10 Y. Chen, J. Wang, H. Liu, M. N. Banis, R. Li, X. Sun, T. K. Sham, S. Ye and S. Knights, *J. Phys. Chem. C*, 2011, **115**, 3769.
11 Y. Chen, J. Wang, H. Liu, R. Li, X. Sun, S. Ye and S. Knights, *Electrochem. Commun.*, 2009, **11**, 2071.
12 Y. M. Lin, K. A. Jenkins, A. Valdes-Garcia, J. P. Small, D. B. Farmer and P. Avouris, *Nano Lett.*, 2009, **9**, 422.
13 N. Tombros, C. Jozsa, M. Popincius, H. T. Jonkman and B. J. van Wees, *Nature*, 2007, **448**, 571.
14 X. Wang, W. Li, Z. Chen, M. Waje and Y. Yan, *J. Power Sources*, 2006, **158**, 154.
15 Y. Shao, G. Yin, Y. Gao and P. Shi, *J. Electrochem. Soc.*, 2006, **153**, A1093.
16 W. Z. Li, C. H. Liang, W. J. Zhou, J. S. Qiu, Z. H. Zhou, G. Q. Sun and Q. Xin, *J. Phys. Chem. B*, 2003, **107**, 6292.
17 E. Durgun, S. Dag, V. M. K. Bagci, O. Gűlseren, T. Yildirim and S. Ciraci, *Phys. Rev. B: Condens. Matter Mater. Phys.*, 2003, **67**, R201401.
18 J. Wang, Y. Lv, X. Li and M. Dong, *J. Phys. Chem. C*, 2009, **113**, 890.
19 Y. H. Li, T. H. Hung and C. W. Chen, *Carbon*, 2009, **47**, 850.
20 W. An and C. H. Turner, *J. Phys. Chem. C*, 2009, **113**, 7069.
21 (*a*) S. Jiang, Y. Ma, G. Jian, H. Tao, X. Wang, Y. Fan, Y. Lu, Z. Hu and Y. Chen, *Adv. Mater.*, 2009, **21**, 4953; (*b*) B. Yue, Y. Ma, H. Tao, L. Yu, G. Jian, X. Wang, X. Wang, Y. Lu and Z. Hu, *J. Mater. Chem.*, 2008, **18**, 1747; (*c*) H. Feng, J. Ma and Z. Hu, *J. Mater. Chem.*, 2010, **20**, 1702.
22 P. G. Collins, K. Bradley, M. Ishigami and A. Zettl, *Science*, 2000, **287**, 1801.
23 T. Y. Kim, K. R. Lee, K. Y. Eun and K. H. Oh, *Chem. Phys. Lett.*, 2003, **372**, 603.
24 M. Burghard and K. Balasubramanian, *Small*, 2005, **1**(2), 180.
25 J. Zhang, H. Zou, Q. Qing, Y. Yang, Q. Li, Z. Liu, X. Guo and Z. Du, *J. Phys. Chem. B*, 2003, **107**(16), 3712.
26 P. Ordejón, E. Artacho and J. M. Soler, *Phys. Rev. B: Condens. Matter Mater. Phys.*, 1996, **53**(16), 10441.
27 J. M. Soler, E. Artacho, J. D. Gale, A. García, J. Junquera, P. Ordejón and D. Sánchez-Portal, *J. Phys.: Condens. Matter*, 2002, **14**(11), 2745.
28 J. P. Perdew, K. Burke and M. Ernzerhof, *Phys. Rev. Lett.*, 1996, **77**(18), 3865.
29 N. Troullier and J. L. Martins, *Phys. Rev. B: Condens. Matter Mater. Phys.*, 1991, **43**(3), 1993.
30 S. F. Boys and F. Bernardi, *Mol. Phys.*, 1970, **19**(4), 553.
31 H. Monkhorst and J. D. Pack, *Phys. Rev. B: Solid State*, 1976, **13**(12), 5188.
32 H. L. Zhuang, G. P. Zheng and A. K. Soh, *Comput. Mater. Sci.*, 2008, **43**, 823.
33 G. Kim and S. H. Jhi, *ACS Nano*, 2011, **5**(2), 805.
34 J. K. Nørskov, T. Bligaard, J. Rossmeisl and C. H. Christensen, *Nat. Chem.*, 2009, **1**, 37–46.

